Vol. 16, No. 2, 2025
ISSN 2233-4203/ e-ISSN 2093-8950
ARTICLE www.msletters.org | Mass Spectrometry Letters

Research and Application of Proton Transfer Reaction Mass Spectrometry in Natural Gas Leakage Detection

Min Ren[1]* and Jian Ren[2]

[1]*College of Electromechanical Engineering, Shanxi Datong University. Shanxi Datong , China*
[2]*College of fine arts, Shanxi Datong University. Shanxi Datong, China*

Received March 21, 2025, Revised June 02, 2025, Accepted June 5, 2025
First published on the web June 30, 2025; DOI: 10.5478/MSL.2025.16.2.52

Abstract : Natural gas has become an indispensable energy source for daily life, but natural gas leakage brings great harm to both residents' life and property as well as the atmospheric environment. The severe harm caused by natural gas leakage can be prevented by taking appropriate measures during the early stages of the leak. In this paper, proton transfer reaction mass spectrometer (PTR-MS) was used to detect the standard gas of simulated natural gas components by using a new reagent ion, CF_3^+ ion. The study demonstrates that CF_3^+ ions can chemically react with ethane in natural gas, resulting in the production of $C_2H_5^+$ and $F^+(C_2H_6)$ ions. By plotting the standard curve, the detection limits of *m/z* 29 and 49 product ions were calculated to be 6.251 μg/m^3 and 6.87 μg/m^3, respectively, with the relative standard deviations (RSDs) ranging from 1.8% to 3.5%. It can fully meet the demand of early trace leakage detection of natural gas, and greatly improve the early warning capability of natural gas leakage, and provide reliable protection of the residents' life and property as well as the atmospheric environment. It also provides a new research method for early warning detection of natural gas leakage.

Keywords : PTR-MS, CF_4, natural gas leakage, ethane

Introduction

Natural gas, as an efficient and clean energy, has become an essential and important energy source in people's daily life and industrial production. At present, the transportation of natural gas in the city is mainly through natural gas pipelines, which are mostly buried underground to ensure the beauty and cleanliness of the city.[1] However, it makes the pipelines particularly susceptible to corrosion, leading to potential natural gas leaks.[2] If natural gas leaks are not detected on time, it can result in significant gas emissions, which may trigger explosions, posing a serious threat to the safety of residents and their property.[3]

Natural gas is composed of multi-component gases, including methane, ethane, propane, etc., of which methane content accounts for more than 95%.[4] The explosive range of natural gas in air is between 5% and 15% by volume, meaning it can ignite immediately upon contact with an open flame or heat source when its concentration falls within this range.[2,5] For instance, according to the 2022 report on natural gas leak incidents in China, a total of 802 gas accidents were reported throughout the year, including 457 incidents involving residential users, 123 incidents involving commercial users, and 212 pipeline incidents, with pipeline accidents accounting for 26.4% of the total. The main causes of pipeline leaks include metal corrosion and valve failures.[6]

In addition, methane is a potent greenhouse gas, ranking as the second-largest contributor to global warming after carbon dioxide. Its greenhouse effect is more than 20 times that of carbon dioxide. Therefore, the leakage of natural gas poses significant risks not only to the safety of residents and their property but also to the atmospheric environment.[7]

Natural gas detection status and methods

Currently, there are several methods for detecting natural gas leakage, which can be divided into two categories based on the detection target:

(1) Detection of Methane: Common methods for methane detection include catalytic combustion,[8] semiconductor sensors,[9] Tunable Diode Laser Absorption Spectroscopy (TDLAS),[10] and gas chromatography.[11] Although these methods are widely used for methane detection, they face several challenges in practical applications.[12] For instance, the catalytic combustion method has high operational diffi-

*Reprint requests to Min Ren
https://orcid.org/0009-0006-4123-9597
E-mail: renmin890123@163.com

culty and detection limits. Semiconductor sensors have a short lifespan and limited usage cycles. TDLAS is prone to interference, and gas chromatography cannot perform real-time continuous monitoring.[13] Additionally, since natural gas pipelines are buried underground, they are particularly susceptible to interference from methane in underground biogas, which can lead to significant disruptions and misjudgments in natural gas leak detection.[14]

(2) Detection of Ethane: As mentioned earlier, urban natural gas pipelines are buried underground, where both biogas and natural gas primarily consist of methane. This often results in false alarms when using methane detection instruments to identify natural gas leaks, wasting human and material resources. Since biogas is mainly composed of methane, nitrogen, ammonia, and carbon dioxide without ethane while natural gas contains ethane, detecting the presence of ethane in the measured gas can help distinguish between biogas and leaking natural gas.[15] Existing ethane detection instruments can qualitatively analyse biogas and natural gas by detecting ethane; however, the testing time is lengthy, with the entire detection and analysis process taking about 5 minutes. Each test requires resampling and analysis, resulting in a long response cycle. Moreover, the instrument has a short battery life and a detection limit of approximately 10 ppm, which does not meet the requirements for early warning of trace natural gas leaks.[16] Additionally, mid-infrared trace ethane sensors have been experimentally calculated to have a minimum detection limit of around 33 ppb, but they have not yet been applied in the detection of trace natural gas leaks.[17]

Among the above methods for natural gas leakage detection, methane detector cannot accurately determine whether the source of methane is caused by natural gas leakage.[18] Ethane detector can determine the ethane from natural gas leakage, but each detection and analysis take about 5 minutes, and then need to be sampled again to detect and analyse.[19] This makes continuous online analysis impossible. In cases involving large-scale and long-distance natural gas pipelines, the instruments have limited battery life and usage duration, with a minimum detection limit of 10 ppm, which is inadequate for effectively detecting early trace leaks of natural gas.[20]

Experimental

Instrument and standard gases

Instrument: PTR-QMS 3500 Proton Transfer Reaction Mass Spectrometer (Beijing East & West Analytical Instruments, China).

Standard gas: CF_4 purity 99.999%.

In order to detect whether CF_3^+ ions can react with C_2H_6 by proton transfer, a standard gas of 122.7 mg/m^3 C_2H_6 was prepared. Since the PTR-MS is aimed at the detection of early trace leakage of natural gas, the following three gradient standard gases were prepared to simulate the early trace leakage of natural gas.

Standard gas I: 64.64 mg/m^3 CH_4, 12.11 mg/m^3 C_2H_6, 18.36 mg/m^3 C_3H_8, 32.19 mg/m^3 C_6H_6.

Standard gas II: 6.58 mg/m^3 CH_4, 1.26 mg/m^3 C_2H_6, 1.84 mg/m^3 C_3H_8, 3.16 mg/m^3 C_6H_6.

Standard gas III: 0.65 mg/m^3 CH_4, 0.12 mg/m^3 C_2H_6, 0.18 mg/m^3 C_3H_8, 0.32 mg/m^3 C_6H_6.

Four bottles of standard gas, the equilibrium gas was nitrogen, and the gas concentrations were all prepared at 0^{o}C and 101.325 kPa. (Dalian Dart Company)

Principle of PTR-MS

PTR-MS is a soft ionization mass spectrometry technique based on chemical ionisation, which has the advantages of direct injection (no sample pre-treatment)[21], short response time (100 ms)[22] and low detection limit (ppt level).[23] Currently, it is widely used in the fields of atmospheric environment detection,[24] public safety,[25] medical diagnosis[26] and food safety.[27,28] In this paper, PTR-MS was used to detect the early trace leakage of natural gas, and to determine whether natural gas is leaking by detecting ethane, especially for the early trace leakage of natural gas.

The prerequisite for the proton transfer reaction to occur depends on the relationship between the proton affinity potential (PA) of the reagent gas and the analysed molecule.[29] The commonly used reagent ion is H_3O^+.[30] In order to ensure that the proton transfer reaction can occur, $H_3O^+ + M \rightarrow MH^+ + H_2O$, the proton affinity potential of the detected substance M must be greater than the proton affinity potential of water.[31,32] The proton affinity potentials of

Table 1. Proton affinity potentials and ionisation energies of common substances

Substance	Molecular formula	Molecular mass	Proton affinity potential (kJ/mol)	Ionisation energy (eV)
Carbon dioxide	CO_2	44.0095	540.5	13.78
Oxygen	O_2	31.9988	421	12.07
Carbon tetrafluoride	CF_4	88.0043	529.3	14.0
Methane	CH_4	16.0425	543.5	12.61
Ethane	C_2H_6	30.069	596.3	11.52
Propane	C_3H_8	44.0956	625.7	10.94
Water	H_2O	18.0153	691	12.62

common substances are shown in Table 1.

From Table 1, it can be seen that the proton affinity of water is greater than that of methane, ethane, and propane. Therefore, traditional H_3O^+ reagent ions are not effective for detecting methane or ethane in natural gas.[33,34] To enable the detection of natural gas through proton transfer reactions, it is necessary to select a new reagent ion.[35] This reagent should readily ionize to form reagent ions, and its proton affinity must be lower than that of methane or ethane. Ultimately, tetrafluoromethane was chosen, as shown in Table 1, where the proton affinity of tetrafluoromethane is lower than that of ethane, indicating that proton transfer reactions can theoretically occur.

Mass Spectrometry Operating Conditions

Reagents: pure CF_4.

Scanning Methods:

(1) Full Scan: To detect new reagent ions, pure CF_4 gas is introduced into the ion source to observe whether reagent ions can be generated, with a scanning range of 10-100 amu.

(2) Detecting whether CF_3^+ ions can react with ethane and produce new product ions.

(3) Selection of ion scanning method. Using CF_3^+ ions to detect the simulated natural gas standard gas, due to the production of more fragment ions, in order to exclude the influence of fragment ions on the detection results, the selective ion scanning method was adopted for *m/z* 29 ($C_2H_5^+$) and *m/z* 49 ($F^+(C_2H_6)$).

Results and Discussion

Figure 1 shows the full spectrum after exciting high-purity CF_4 gas. Since the ion source operates in an environment of approximately 100 Pa, a small amount of air is mixed in the ion source. From the spectrum it can be seen that a total of five ions of *m/z* 19, 30, 32, 46, and 69 are produced. The *m/z* = 19 (H_3O^+ or F^+), due to the dry air, there is very little moisture in it, so the H_3O^+ ions should be minimal, and most of the *m/z* 19 is F^+ produced by the ionisation of CF_4. *m/z* = 30 (NO^+), *m/z* = 32 (O_2^+), *m/z* = 46 (NO_2^+) is from nitrogen and oxygen in the air. *m/z* 69 is CF_3^+ ions, and the content is very high, it can be confirmed that CF_4 ionisation produced a large number of CF_3^+ ions. Figure 1 clearly demonstrates that CF_4 can be used as a new reagent and can generate a new reagent ion, CF_3^+.

From Figure 1, it can be confirmed that new reagent ions CF_3^+ can be produced. To test whether CF_3^+ ions can undergo proton transfer reactions with ethane, a standard gas of ethane at a concentration of 122.7 mg/m³ was passed into the drift tube. Figure 2 displays the full mass spectrum acquired from PTR-MS analysis of ethane, highlighting characteristic fragment ions and major peaks. Compared to Figure 1, Figure 2 shows a significant increase in the number of ion peaks. The main ion peaks are *m/z* 12, 26, 27, 28, 29, 30, 31, 38, 49, 53, and 69. of which except for *m/z* 19 and 69 which are obtained in Figure. 1. This indicates that the CF_3^+ ion reacts with ethane in a series of reactions to produce a variety of ion products.

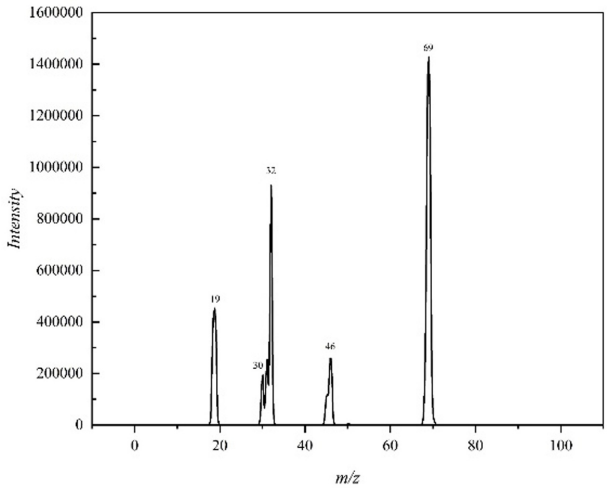

Figure 1. Mass spectrum of excited pure CF_4.

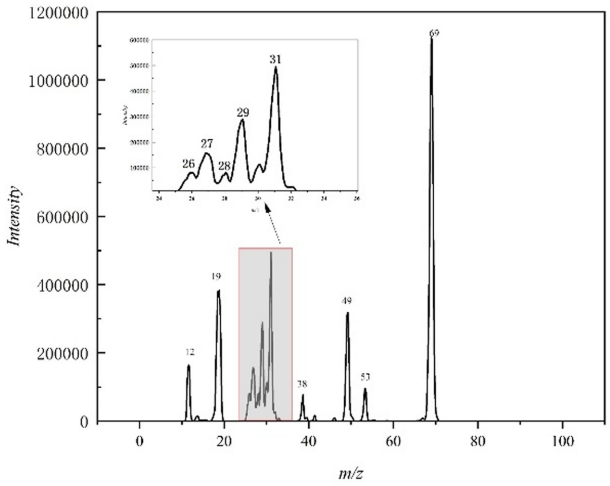

Figure 2. Mass spectrum of 122.7 mg/m^3 ethane detected by PTR-MS.

Notably, *m/z* 12 corresponds to C^+ ions. From Figure 1, it is evident that no C^+ ions were produced during the excitation of CF_4, suggesting that C^+ ions are fragment ions generated from the collision reaction between CF_3^+ ions and ethane. Since the ionization energy of CF_3^+ is about 11.5eV, CF_3^+ and ethane can have a charge exchange reaction, which theoretically produces $C_2H_6^+$, but in the actual collision process, due to the different collision positions and angles. *m/z* 26 ($C_2H_2^+$), 27 ($C_2H_3^+$), 28 ($C_2H_4^+$), and 29 ($C_2H_5^+$) fragment ions were produced.

Additionally, due to interference from NO^+ ions in the air,

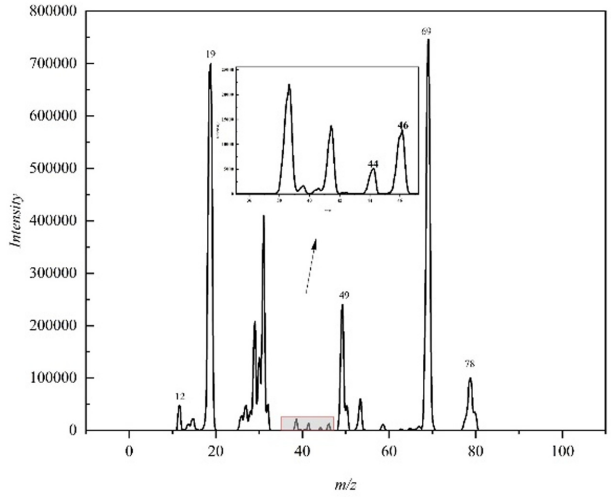

Figure 3. Mass spectrum of standard gas I detected by PTR-MS.

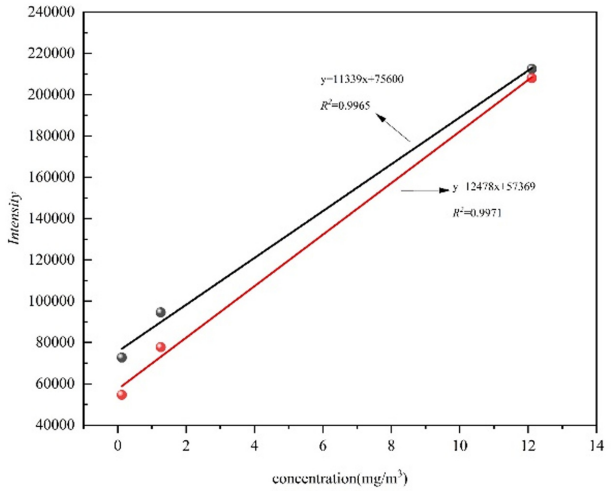

Figure 4. Relationship between ethane concentration and *m/z* 29 and 49 ion peak intensities.

m/z 30 cannot be used as a standard peak for detecting ethane. *m/z* 31 is CF^+ ion, *m/z* 38 is F_2^+, *m/z* 49 is a mixed ion peak of F^+ (C_2H_6) and H_3O^+ (C_2H_6) produced by the clustering reaction of F^+ with C_2H_6, which are bound ethane molecules, although interfering peaks are present. The *m/z* 53 peak is a fragment interference ion. Therefore, CF_3^+ ions can effectively detect ethane.

Figure 2 demonstrates that CF_3^+ ions can be used to detect ethane. In order to test the effectiveness of CF_3^+ ions in detecting natural gas leaks, the full spectrum of simulated natural gas standard gas I was detected using CF_3^+ ions, as shown in Figure 3. From the figure, it can be seen that in addition to the ion peaks appearing in the detection of ethane as in Figure. 2, the ion peaks of *m/z* 44, 46, and 78 also appeared. Since the ionization energy of propane is lower than that of ethane, CF_3^+ ions and propane can also undergo a charge exchange reaction to produce $C_3H_8^+$ ion. Therefore, the peak at *m/z* 44 is assigned to the $C_3H_8^+$ ion. Since benzene is added to the standard gas, the CF_3^+ ion undergoes a charge exchange reaction with benzene to produce *m/z* 78 ($C_6H_6^+$).

From Figure 3, it can be seen that CF_3^+ can detect not only ethane, but also a small amount of propane for the standard gas that simulates natural gas. It is entirely possible to detect natural gas using CF_3^+ ions.

Limit of detection

Early trace leakage detection of natural gas can be achieved by detecting ethane using PTR-MS. In order to determine the detection limit of PTR-MS for ethane, three concentrations of ethane, 12.11 mg/m^3, 1.26 mg/m^3, and 0.12 mg/m^3, were tested. The peak intensities for *m/z* 29 and 49 were measured and recorded, and the slopes of the fitted curves were calculated, as shown in Figure 4. The red curve corresponds to the m/z 29 ion, with the equation y = 12478x + 57369 and R^2 = 0.9971. The black curve corresponds to the *m/z* 49 ion, with the equation y = 11339x + 75600 and R^2 = 0.9965.

Under the same mass spectrometry conditions, high-purity nitrogen gas was continuously sampled 11 times, and the $C_2H_5^+$ mass spectrum peak heights were recorded as blanks. The standard deviation of the blank was calculated based on these measurements, and the detection limit was then calculated using the appropriate formula.

$$D_L = \frac{3s_B}{C}$$

Format:

D_L: Limit of detection;

s_B: standard deviation of 11 consecutive measurement blanks;

C: slope of the fitted standard curve.

From the analysis of the measurements, the standard deviation of the blank for 11 consecutive measurements was calculated to be about 26. The slope of the fitted standard curve was about 12478. So the detection limit for ethane:

$$D_L = \frac{3S_B}{C} = \frac{3 \times 26}{12478} = 6.251 \ \mu g/m^3$$

Using the same method, the detection limit of ethane was 6.87 μg/m^3 when the *m/z* 49 ion peak was recorded.

Therefore, whether detecting ethane ions at *m/z* 29 or 49, the detection limit reaches the μg/m^3 level, which is sufficient to fully meet the requirements for trace detection.

Precision

Daily inspection of natural gas pipelines is long distance, long duration, and also need to consider the influence of the surrounding environment, so in order to detect the precision

Table 2. Results of the relative standard deviations (RSD) of ethane detection by PTR-MS (n = 10)

Ion	Test value/(cps)										Average (n = 10) (cps)	RSD (n = 10) %
$C_2H_5^+$	212475	212508	212487	212493	212398	212454	212512	212496	212429	212436	212468	1.8
$F^+(C_2H_6)$	208029	208106	207989	208043	207945	208087	208124	208092	207895	208042	208035	3.5

of the instrument, by allowing the instrument to run continuously for 24 h, in the process of arbitrarily selecting 10 time points to detect 12.11 mg/m^3 ethane, according to the above method to detect the precision of the instrument. The precision of the instrument was tested by checking the signal strength at *m/z* 29 and 49. The relative standard deviations were calculated to be 1.8% to 3.5% based on the results of 10 detections and the average values, as shown in Table 2. The results show that the detection of natural gas leakage using PTR-MS is accurate and reliable with high precision, which meets the detection requirements.

Conclusions

The proton transfer reaction mass spectrometer was used employing the new reagent ion CF_3^+ for ionization. The CF_3^+ ion was used to detect ethane to achieve the early trace leakage detection of natural gas, and the detection limit can reach μg/m^3 level with the relative standard deviation (RSD) of 1.8% to 3.5%. Meanwhile, PTR-MS has the advantages of direct injection, no sample pre-treatment, short response time and unlimited sampling mode, which can fully meet the needs of urban natural gas pipeline, long distance, trace leakage detection, and provides a rapid and accurate detection method for early trace leakage detection of natural gas.

Acknowledgments

This work was supported by Shanxi Datong University Yungang Special Project [2020YGZX092] and Shanxi Datong University Yungang Studies Special Project[2023YGYB12].

References

1. Reymond, M. *Energy Policy* **2007**, 35, 4169. https://doi.org/10.1016/j.enpol.2007.02.030.
2. Li, C.J.; Zhang, Y.R.; Jia, W.L.; Hu, X.Y.; Song, S.S.; Yang, F. *Gas Sci. Eng.* **2024**, 122. https://doi.org/10.1016/j.jgsce.2023.205187.
3. Zimmerle, D.; Vaughn, T.; Bell, C.; Bennett, K.; Deshmukh, P.; Thoma, E. *Environ. Sci. Technol.* **2020**, 54, 11506. https://doi.org/10.1021/acs.est.0c01285.
4. Liang, J.; Ma, L.; Liang, S.; Zhang, H.; Zuo, Z.L.; Dai, J. *Comput. Electr. Eng.* **2023**, 110. https://doi.org/10.1016/j.compeleceng.2023.108833.
5. Li, G.; Zeng, K.H.; Zhou, B.; Yang, W.M.; Lin, X.H.; Wang, F.; Chen, Y.T.; Ji, X.T.; Zheng, D.H.; Mao, B.M. *Instrum. Sci. Technol.* **2021**, 49, 65. https://doi.org/10.1080/10739149.2020.1780253.
6. Lukonge, A.B.; Cao, X.W. *Trans. Indian Inst. Met.* **2020**, 73, 1715. https://doi.org/10.1007/s12666-020-02002-x.
7. Scheitrum, D.; Jaffe, A.M.; Dominguez-Faus, R.; Parker, N. *Energy Policy* **2017**, 110, 355. https://doi.org/10.1016/j.enpol.2017.08.034.
8. Wang, H.R.; Zhang, W.; You, L.D.; Yuan, G.Y.; Zhao, Y.L.; Jiang, Z.D. *Instrum. Sci. Technol.* **2013**, 41, 608. https://doi.org/10.1080/10739149.2013.816965.
9. Ma, L.; Liu, X.; Si, G.S. *Sensors* **2024**, 24. https://doi.org/10.3390/s24155031.
10. Lomond, J.S.; Tong, A.Z. *J. Chromatogr. Sci.* **2011**, 49, 469. https://doi.org/10.1093/chrsci/49.6.469.
11. Sneddon, J.; Masuram, S.; Richert, J.C. *Anal. Lett.* **2007**, 40, 1003. https://doi.org/10.1080/00032710701300648.
12. Kemp, C.E.; Ravikumar, A.P.; Brandt, A.R. *Environ. Sci. Technol.* **2016**, 50, 4546. https://doi.org/10.1021/acs.est.5b06068.
13. Kamieniak, J.; Randviir, E.P.; Banks, C.E. *TrAC, Trends Anal. Chem.* **2015**, 73, 146. https://doi.org/10.1016/j.trac.2015.04.030.
14. Müller, M.; Piel, F.; Gutmann, R.; Sulzer, P.; Hartungen, E.; Wisthaler, A. *Int. J. Mass Spectrom.* **2020**, 447. https://doi.org/10.1016/j.ijms.2019.116254.
15. Santosa, I.E.; Laarhoven, L.J.J.; Harbinson, J.; Driscoll, S.; Harren, F.J.M. *Rev. Sci. Instrum.* **2003**, 74, 680. https://doi.org/10.1063/1.1512772.
16. Oh, M.K.; Lee, Y.H.; Choi, S.C.; Ko, D.K.; Lee, J.M. *J. Opt. Soc. Korea* **2008**, 12, 1. https://doi.org/10.3807/josk.2008.12.1.001.
17. Yu-quan, Z.H.U.; Li-feng, Q.; Qi-xing, Z.; Ting-li, C.A.I.; Jin-jun, W.; Yong-ming, Z. *Journal of University of Science and Technology of China* **2009**, 39, 429.
18. Hou, Q.M. *Math. Probl. Eng.* **2021**, 2021. https://doi.org/10.1155/2021/5548503.
19. Murvay, P.S.; Silea, I. *Journal of Loss Prevention in the Process Industries* **2012**, 25, 966. https://doi.org/10.1016/j.jlp.2012.05.010.
20. Zuo, Z.L.; Zhang, H.; Ma, L.; Liu, T.; Liang, S. *IEEE Trans. Ind. Electron. Control Instrum.* **2024**, 71, 6263. https://doi.org/10.1109/tie.2023.3294645.
21. Wang, Y.J.; Dong, K.X.; Chu, Y.N. *Instrum. Sci. Technol.* **2019**, 47, 410. https://doi.org/10.1080/10739149.2019.1579100.
22. Pan, Y.; Zhang, Q.L.; Zhou, W.Z.; Zou, X.; Wang, H.M.; Huang, C.Q.; Shen, C.Y.; Chu, Y.N. *J. Am. Soc. Mass Spectrom.* **2017**, 28, 873. https://doi.org/10.1007/s13361-017-1638-7.

23. Yuan, B.; Koss, A.R.; Warneke, C.; Coggon, M.; Sekimoto, K.; de Gouw, J.A. *Chem. Rev.* **2017**, 117, 13187. https://doi.org/10.1021/acs.chemrev.7b00325.
24. Biasioli, F.; Gasperi, F.; Odorizzi, G.; Aprea, E.; Mott, D.; Marini, F.; Autiero, G.; Rotondo, G.; Märk, T.D. *Int. J. Mass Spectrom.* **2004**, 239, 103. https://doi.org/10.1016/j.ijms.2004.07.024.
25. Zhang, Q.L.; Zou, X.; Liang, Q.; Wang, H.M.; Huang, C.Q.; Shen, C.Y.; Chu, Y.N. *J. Am. Soc. Mass Spectrom.* **2019**, 30, 501. https://doi.org/10.1007/s13361-018-2108-6.
26. Aprea, E.; Biasioli, F.; Carlin, S.; Versini, G.; Märk, T.D.; Gasperi, F. *Rapid Commun. Mass Spectrom.* **2007**, 21, 2564. https://doi.org/10.1002/rcm.3118.
27. Biasioli, F.; Yeretzian, C.; Gasperi, F.; Märk, T.D. *TrAC, Trends Anal. Chem.* **2011**, 30, 968. https://doi.org/10.1016/j.trac.2011.03.009.
28. Franke, C.; Beauchamp, *J. Food Anal. Method.* **2017**, 10, 310. https://doi.org/10.1007/s12161-016-0585-4.
29. Knighton, W.B.; Herndon, S.C.; Franklin, J.F.; Wood, E.C.; Wormhoudt, J.; Brooks, W.; Fortner, E.C.; Allen, D.T. *Ind. Eng. Chem. Res.* **2012**, 51, 12674. https://doi.org/10.1021/ie202695v.
30. Yu, Z.J.; Liu, C.; Niu, H.Z.; Wu, M.M.; Gao, W.; Zhou, Z.; Huang, Z.X.; Li, X. *Analytical Methods* **2020**, 12, 4343. https://doi.org/10.1039/d0ay01102a.
31. Liang, Q.; Bao, X.; Sun, Q.; Zhang, Q.L.; Zou, X.; Huang, C.Q.; Shen, C.Y.; Chu, Y.N. *Environmental Pollution* **2020**, 265. https://doi.org/10.1016/j.envpol.2020.114628.
32. Zou, X.; Kang, M.; Wang, H.M.; Huang, C.Q.; Shen, C.Y.; Chu, Y.N. *Chemosphere* **2017**, 177, 217. https://doi.org/10.1016/j.chemosphere.2017.02.141.
33. Sekimoto, K.; Koss, A.R. *J. Mass Spectrom.* **2021**, 56. https://doi.org/10.1002/jms.4619.
34. González-Méndez, R.; Reich, D.F.; Mullock, S.J.; Corlett, C.A.; Mayhew, C.A. *Int. J. Mass Spectrom.* **2015**, 385, 13. https://doi.org/10.1016/j.ijms.2015.05.003.
35. Müller, M.; Piel, F.; Gutmann, R.; Sulzer, P.; Hartungen, E.; Wisthaler, A. *Int. J. Mass Spectrom.* **2020**, 447. https://doi.org/10.1016/j.ijms.2019.116254.